THE JOURNAL OF BIOLOGICAL CHEMISTRY VOL. 289, NO. 22, pp. 15856–15866, May 30, 2014

Allosteric Modulation of M_1 Muscarinic Acetylcholine Receptor Internalization and Subcellular Trafficking*

Received for publication, November 20, 2013, and in revised form, April 14, 2014 Published, JBC Papers in Press, April 21, 2014, DOI 10.1074/jbc.M113.536672

Holly R. Yeatman[‡], J. Robert Lane[‡1], Kwok Ho Christopher Choy[‡], Nevin A. Lambert[§], Patrick M. Sexton[‡2], Arthur Christopoulos[‡2,3], and Meritxell Canals[‡4]

From the [‡]Drug Discovery Biology, Monash Institute of Pharmaceutical Sciences, Faculty of Pharmacy and Pharmaceutical Sciences, Monash University, Parkville, Melbourne, Victoria 3052, Australia and [§]Department of Pharmacology and Toxicology, Georgia Regents University, Augusta, Georgia 30912

Background: The effects of allosteric modulators on G protein-coupled receptor trafficking are largely unknown.
Results: The allosteric ligand BQCA modulates M_1 mAChR arrestin recruitment and receptor trafficking.
Conclusion: M_1 mAChR trafficking is arrestin- and G protein-dependent and modulated by BQCA.
Significance: The impact of allosteric modulators on receptor trafficking needs to be assessed when considering this family of ligands as potential chronic therapies.

Allosteric modulators are an attractive approach to achieve receptor subtype-selective targeting of G protein-coupled receptors. Benzyl quinolone carboxylic acid (BQCA) is an unprecedented example of a highly selective positive allosteric modulator of the M_1 muscarinic acetylcholine receptor (mAChR). However, despite favorable pharmacological characteristics of BQCA *in vitro* and *in vivo*, there is limited evidence of the impact of allosteric modulation on receptor regulatory mechanisms such as β-arrestin recruitment or receptor internalization and endocytic trafficking. In the present study we investigated the impact of BQCA on M_1 mAChR regulation. We show that BQCA potentiates agonist-induced β-arrestin recruitment to M_1 mAChRs. Using a bioluminescence resonance energy transfer approach to monitor intracellular trafficking of M_1 mAChRs, we show that once internalized, M_1 mAChRs traffic to early endosomes, recycling endosomes and late endosomes. We also show that BQCA potentiates agonist-induced subcellular trafficking. M_1 mAChR internalization is both β-arrestin and G protein-dependent, with the third intracellular loop playing an important role in the dynamics of β-arrestin recruitment. As the global effect of receptor activation ultimately depends on the levels of receptor expression at the cell surface, these results illustrate the need to extend the characterization of novel allosteric modulators of G protein-coupled receptors to encapsulate the consequences of chronic exposure to this family of ligands.

Muscarinic acetylcholine (ACh)[5] receptors (mAChRs) are an important subfamily of class A G protein-coupled receptors (GPCRs). Of the five mAChR subtypes, the M_1 mAChR has attracted particular attention for the treatment of several CNS disorders (1, 2). The M_1 mAChR couples predominantly to $G\alpha_{q/11}$ G proteins, leading to phospholipase Cβ-mediated hydrolysis of phosphatidylinositol-4,5-bisphosphate and subsequent calcium mobilization from intracellular stores (3). In the brain the M_1 mAChR is concentrated in forebrain structures such as the frontal cortex and hippocampus, where it is implicated in memory processing and cognition (4), and as such, M_1 mAChRs have been suggested as a target for the development of cognitive enhancers for conditions such as Alzheimer disease (5). Unfortunately, achieving subtype selectivity at mAChRs is challenging given the highly conserved nature of the orthosteric site across the mAChR family. Despite considerable efforts, only moderately selective orthosteric ligands have been developed (1). Increased subtype selectivity has been achieved by recent progress in the development of allosteric ligands, which bind to a topographically distinct site from the orthosteric site. An exemplar molecule in this regard is the M_1 mAChR-selective allosteric modulator, benzyl quinolone carboxylic acid (BQCA), which exhibits *in vivo* efficacy as a potentiator of ACh and has the potential to ameliorate impairments in cognitive function (6, 7). In a recent mechanistic study, we found that interaction between BQCA and the M_1 mAChR is consistent with a two-state model of receptor activation (8) whereby BQCA exhibits positive cooperativity with orthosteric agonists but negative cooperativity with inverse agonists in a manner that correlates with orthosteric ligand efficacy and stimulus-response coupling of the receptor (8). Additionally, BQCA does not engender pathway-biased signaling by orthosteric agonists at the M_1 mAChR (8). These prop-

* This work was supported by National Health and Medical Research Council Program Grant 519461 (to A. C. and P. M. S.) and Project Grant APP1011796 (to M. C.).

[1] A Career Development Fellow of the National Health and Medical Research Council of Australia.
[2] A Principal Research Fellow of the National Health and Medical Research Council of Australia.
[3] To whom correspondence may be addressed. Tel.: 613-9903-9067; Fax: 613-9903-9581; E-mail: arthur.christopoulos@monash.edu.
[4] A Monash Research Fellow. To whom correspondence may be addressed. Tel.: 613-9903-9094; Fax: 613-9903-9581; E-mail: meri.canals@monash.edu.

[5] The abbreviations used are: ACh, acetylcholine; mAChR, muscarinic acetylcholine receptor; GPCR, G protein-coupled receptor; GRK, GPCR kinase; BQCA, benzyl quinolone carboxylic acid; [^{3}H]NMS, N-[^{3}H]methylscopolamine; CCh, carbachol; BRET, bioluminescence resonance energy transfer, ICL3, intracellular loop 3; LY2033298, 3-amino-5-chloro-6-methoxy-4-methyl-thieno[2,3-b]pyridine-2-carboxylic acid cyclopropamide.

erties make BQCA a very useful chemical tool with which to probe basic allosteric mechanisms at the M_1 mAChR as a model for general understanding of allostery at GPCRs. However, although the acute signaling profiles of M_1 mAChR allosteric ligands have been extensively characterized (8–10), the understanding of their impact on longer term receptor regulatory processes is currently limited in scope, and some reports to date are contradictory (11). Yet, understanding such processes is vital as most drug therapies involve chronic administration.

Upon activation, GPCRs are rapidly phosphorylated within intracellular loop 3 (ICL3) or the C-terminal tail either by second messenger kinases (such as PKA or PKC) or by GPCR kinases (GRKs). Phosphorylation of the receptor increases its affinity for the scaffolding protein β-arrestin, binding of which prevents further G protein-mediated signaling (12). Once β-arrestins associate with a GPCR, they scaffold the receptor to components of the clathrin-dependent endocytic machinery and promote receptor internalization. The two isoforms of β-arrestin (β-arrestin-1 and 2) interact with multiple intracellular signaling partners such as MAPKs, protein kinase B/Akt, and protein phosphatases such as protein phosphatase 2A (13) and accordingly can also scaffold the receptor to distinct G protein-independent signaling pathways. Dissociation of β-arrestin from the GPCR occurs either at the cell surface or within endosomes, and the dynamics of such uncoupling have a profound impact on the subsequent fate of the desensitized receptor (14).

Here we show that M_1 mAChR internalization is both β-arrestin and G protein-dependent and that the third intracellular loop plays an important role in the dynamics of β-arrestin recruitment. We also exploit the unique properties of BQCA as a tool with which to systematically investigate the impact of allosteric modulation on M_1 mAChR trafficking and regulatory mechanisms. We show that BQCA potentiates agonist-induced β-arrestin recruitment to M_1 mAChRs and receptor endocytosis. Once internalized, M_1 mAChRs traffic to early endosomes, recycling endosomes and late endosomes. BQCA does not alter these trafficking profiles. However, we show for the first time that BQCA potentiates the trafficking of receptors within the different endocytic compartments. These results provide a framework to extend the characterization of allosteric modulators from acute signaling events into receptor regulatory processes, a dimension that must be investigated when considering the chronic use of these ligands.

EXPERIMENTAL PROCEDURES

Materials—Dulbecco's modified Eagle's medium, Hanks' balanced salt solution, FlpIn Chinese hamster ovary (CHO) cells, penicillin/streptomycin, ProLong Gold, and Fluo-4-AM were purchased from Invitrogen. HygroGold was purchased from InvivoGen (San Diego, CA). Fetal bovine serum was purchased from In Vitro Technologies (Noble Park, VIC, Australia). Polyethyleneimine was from Polysciences (Warrington, PA). *N*-[^{3}H]Methylscopolamine ([^{3}H]NMS) and Optiphase scintillation mixture were from PerkinElmer Life Sciences. Coelenterazine h was purchased from Promega (Alexandria, NSW, Australia). Dynasore was purchased from Tocris Bioscience (Bristol, UK). Pitstop2 was purchased from Abcam (Cambridge, MA). UBO-QIC was purchased from the Institute of Pharmaceutical Biology, University of Bonn (Germany). All other reagents were purchased from Sigma. BQCA was synthesized in-house.

YFP-β-arrestin-1 and 2 constructs were gifts from Marc Caron (Duke University). Venus-Rab5a, Rab7a, and Rab11 constructs were generated as previously described (15). The M_1 R123L mAChR mutation was generated using the QuikChange site-directed mutagenesis kit (Agilent Technologies, La Jolla, CA) following the manufacturer's instructions. p416GPD-M_1Δi3 was a gift from Jürgen Wess (NIDDK, National Institutes of Health). The M_1, M_1R123L, and M_1Δi3-Rluc8 constructs were generated by replacement of the stop codon with a NotI linker followed by fusion of the cDNA in-frame to Rluc8 in pcDNA3.1.

Cell Culture and Transfections—FlpIn CHO cells stably expressing the WT, Δi3, or R123L hM_1 mAChRs were generated and cultured as described previously (16). Transient transfections of adherent HEK293 cells were performed using linear polyethyleneimine (molecular mass, 25 kDa) in a 1:6 ratio (8).

Inositol 1-Phosphate Accumulation—Inositol 1-phosphate production in M_1 mAChR FlpIn CHOs was measured using the IP-One assay kit (Cisbio) as described previously (17). Data were normalized to the maximum response generated by carbachol (CCh) alone.

Calcium Mobilization—M_1 mAChR FlpIn CHO cells were cultured overnight in 96-well plates at 37 °C in 5% CO_2. Cells were washed twice in Ca^{2+} assay buffer (150 mM NaCl, 2.6 mM KCl, 1.2 mM $MgCl_2$, 10 mM glucose, 10 mM HEPES, 2.2 mM $CaCl_2$, 0.5% (w/v) BSA, and 4 mM probenecid) then incubated in assay buffer containing 1 μM Fluo-4-AM for 1 h at 37 °C in 5% CO_2. Ligands were added, and the fluorescence was quantified in a Flexstation (Molecular Devices, Sunnyvale, CA) using 485-nm excitation and 520-nm emission wavelengths. The peak height of calcium fluorescence was calculated in SoftMax Pro (Molecular Devices) and used in subsequent statistical analyses.

Radioligand Binding—Cells were plated at 20,000 per well in a 96-well Isoplate (PerkinElmer Life Sciences) and allowed to adhere for at least 16 h. Cells were washed 3 times with binding buffer (146 mM NaCl, 10 mM D-glucose, 5 mM KCl, 1 mM $MgSO_4$, 2 mM $CaCl_2$, 1.5 mM $NaHCO_3$, 10 mM HEPES, pH 7.45) and incubated overnight with 4 nM [^{3}H]NMS (specific activity 85.5 mmol/Ci) at 4 °C; any nonspecific binding was determined by the co-addition of 10 μM atropine. For saturation binding assays, cells were incubated overnight at 4 °C with increasing concentrations of [^{3}H]NMS. After washing in cold saline, bound [^{3}H]NMS was solubilized in Optiphase scintillant, and radioactivity was measured in a MicroBeta counter (PerkinElmer Life Sciences).

ELISA—HEK293 cells were transfected with 5 μg of c-myc-hM_1 or empty vector. 24 h post-transfection, cells were plated in poly-D-lysine-coated 48-well culture plates, allowed to adhere, and then grown overnight in serum-free media containing antibiotics. Cells were pretreated with cycloheximide (10 μg/ml) in serum-free media for 30 min before the addition of ligands, which were prepared in cycloheximide-containing media. Inhibitors of internalization were applied during the

pretreatment period and throughout ligand application. To assess receptor recycling, cells were thoroughly washed after ligand incubation, and fresh serum-free medium containing cycloheximide was re-applied. Inhibitors of recycling, where used, were applied from pretreatment through to the end of the washout step. At the conclusion of the incubation period, cells were washed gently 3 times with TBS and fixed in 3.7% v/v paraformaldehyde. Surface or total myc-hM_1 receptors were detected in intact or (Nonidet P-40 equivalent)-detergent permeabilized cells, respectively, using the 9E10 mouse anti-myc antibody (1:2000) followed by HRP-conjugated goat anti-mouse IgG (1:2000). After washing with TBS, the peroxidase substrate (SIGMA*FAST*™ OPD) was added at a final concentration of 0.4 mg/ml, and the reaction was terminated by the addition of 1 M HCl. The colored reaction product was detected at 490 nm in a multi-label plate reader (EnVision, PerkinElmer Life Sciences). The absorbance values for transfected cells were normalized to those of mock-transfected cells, and receptor density was reported relative to vehicle-treated wells.

Bioluminescence Resonance Energy Transfer (BRET)—HEK293 cells were transfected with 1 μg of Rluc8-tagged M_1 and 4 μg of YFP-β-arrestin or 0.5 μg of Rluc8-tagged M_1 and 2 μg of Venus-Rab5a, Rab7a, or Rab11. Twenty-four hours post-transfection, cells were plated in poly-D-lysine-coated 96-well CulturPlates (PerkinElmer Life Sciences) and grown overnight. Cells were allowed to equilibrate in Hanks' balanced salt solution containing 0.05% w/v bovine serum albumin at 37 °C in the presence or absence of specific inhibitors. For kinetic experiments, coelenterazine h was added at a final concentration of 5 μM, and BRET readings were immediately captured using a LUMIstar Omega instrument (BMG LabTech, Offenburg, Germany) that allows for sequential integration of the signals detected at 475 ± 30 and 535 ± 30 nm using filters with the appropriate band pass. Ligands or vehicle were then added after two to four base-line readings. Data are presented as a BRET ratio, calculated as the ratio of YFP to Rluc8 signals and corrected for vehicle. Alternatively, for end point experiments, coelenterazine h was added 10 min before BRET detection, and ligands were added at various time points as described under "Results." End point assay data are reported in milli-BRET units corrected for vehicle.

Immunocytochemistry and Confocal Microscopy—HEK293 cells growing on poly-D-lysine-coated glass coverslips were transfected with 1 μg of c-myc-M_1. After 48 h, cells were incubated with or without ligands (10 μM) for 4 h in the presence of 10 μg/ml cycloheximide. Cells were washed in phosphate-buffered saline (PBS), pH 7.4, fixed in 4% paraformaldehyde in PBS, and then incubated in blocking buffer (3% v/v normal goat serum, 0.1% Triton X-100 in PBS). Primary antibody (9E10, 2 μg/ml) was applied in blocking buffer at 4 °C overnight. Secondary antibody (Alexa-Fluor 594-conjugated goat anti-mouse IgG) was applied for 1 h at room temperature. Coverslips were mounted with ProLong Gold. Images were captured using a Leica TCS SP8 laser scanning confocal microscope (North Ryde, NSW, Australia).

Data Analysis—Data analysis was performed using GraphPad Prism v. 6.0. All affinity and potency values were estimated as logarithms (18). Concentration-response curves for the interaction between allosteric and orthosteric ligands were globally fitted to the following operational model of allosterism and agonism (19),

$$E = \frac{E_m(\tau_A[A](K_B + \alpha\beta[B]) + \tau_B[B]K_A)^n}{([A]K_B + K_AK_B + [B]K_A + \alpha[A][B])^n + (\tau_A[A](K_B + \alpha\beta[B]) + \tau_B[B]K_A)^n} \quad \text{(Eq. 1)}$$

where E_m is the maximum possible cellular response, [A] and [B] are the concentrations of orthosteric and allosteric ligands, respectively, K_A and K_B are the equilibrium dissociation constant of the orthosteric and allosteric ligands, respectively, τ_A and τ_B are operational measures of orthosteric and allosteric ligand efficacy (which incorporate both signal efficiency and receptor density), respectively, α is the binding cooperativity parameter between the orthosteric and allosteric ligand, and β denotes the magnitude of the allosteric effect of the modulator on the efficacy of the orthosteric agonist.

Data are reported as the mean ± S.E., and statistical comparisons between values were by Student's *t* test or analysis of variance with Tukey's multiple comparison post-test as appropriate. A value of $p < 0.05$ was considered statistically significant.

RESULTS

β-Arrestin-2 Recruitment to the M_1 mAChR Is GRK2 and $G\alpha_q$-dependent—We investigated the recruitment of β-arrestins to the M_1 mAChR using BRET. To quantitatively assess the interactions between M_1 mAChRs and β-arrestin-1 or β-arrestin-2, cells were co-transfected with Rluc8-tagged M_1 mAChR and YFP-tagged β-arrestins. Kinetic BRET measurements revealed that stimulation with 1 mM CCh led to a rapid increase in the association of the M_1 mAChR with β-arrestin-2 (Fig. 1*A*). Subsequent addition of the orthosteric antagonist, atropine (10 μM), immediately inhibited the energy transfer between the M_1 mAChR and β-arrestin-2 (Fig. 1*A*). As the BRET signal had reached its maximum after 5 min of incubation with CCh, we constructed concentration-response curves at this time point. M_1 mAChR activation induced a concentration-dependent recruitment of β-arrestin-1 and β-arrestin-2 (Fig. 1*B*). Interestingly, the E_{max} of β-arrestin-1 recruitment was significantly lower than that of β-arrestin-2. Although this difference could be due to a true preference for β-arrestin-2 over β-arrestin-1, this effect can also be explained by different conformations or dipole orientations of the two β-arrestin-YFP proteins, resulting in different energy transfer efficiencies.

Phosphorylation of serine and threonine residues in GPCRs by GRKs, such as GRK2, increases the affinity of the receptor for β-arrestins. Previous studies using purified proteins or overexpression of dominant negative constructs have suggested a role for GRK2 in M_1 mAChR phosphorylation (20–22). CCh-induced recruitment of YFP-β-arrestin-2 to M_1-Rluc8 was attenuated when cells were preincubated with the GRK2 inhibitor 103A (23), resulting in reductions in both potency and E_{max} (Fig. 1*C*). Thus, β-arrestin-2 recruitment to the M_1 mAChR is partially dependent on phosphorylation of the receptor by GRK2.

It is also well accepted that β-arrestin recruitment to GPCRs can occur in the absence of G protein coupling (24). However,

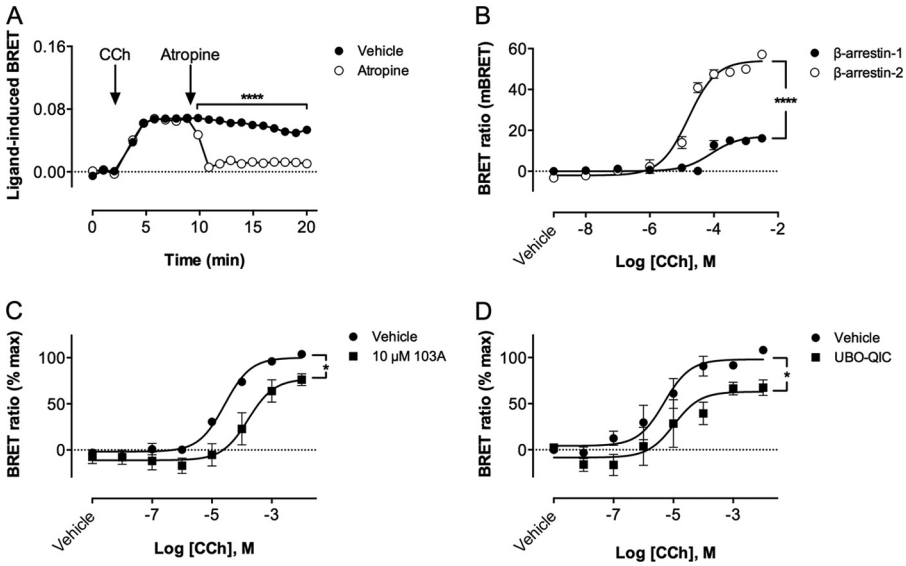

FIGURE 1. **β-Arrestin recruitment at the M_1 mAChR.** *A*, kinetics of CCh-induced YFP-β-arrestin-2 recruitment to hM_1-Rluc8 and antagonism of recruitment by atropine (10 μM, *open symbols*). Ligands were added at the times indicated, and BRET was measured continuously in kinetic mode. Kinetic profiles are a representative experiment performed in triplicate from $n = 2$. *Asterisks* indicate a significant difference between control and atropine-treated cells (****, $p < 0.0001$). *B*, concentration-response curves performed at 5 min for CCh-induced recruitment of YFP-β-arrestin-1 (*filled circles*) and YFP-β-arrestin-2 (*open circles*) to hM_1-Rluc8. $n = 2$. *Asterisks* indicate significant difference in E_{max} (****, $p < 0.0001$). *C*, the GRK2 inhibitor 103A (10 μM) significantly reduced CCh potency and efficacy in a β-arrestin-2 BRET assay. $n = 4$. The *asterisk* indicates significant difference in potency and E_{max} (*, $p < 0.05$). *D*, preincubation with the $G\alpha_q$ inhibitor UBO-QIC (100 nM) significantly reduced maximum CCh-induced β-arrestin-2 recruitment to the M_1 mAChR (*, $p < 0.05$). $n = 3$.

inhibition of $G\alpha_q$ with the specific inhibitor UBO-QIC reduced the maximum recruitment of β-arrestin-2 by 35% (Fig. 1*D*), suggesting that for the M_1 mAChR, β-arrestin recruitment is also G protein-dependent.

We have previously described an ICL3 deletion M_1 mAChR ($M_1\Delta i3$ mAChR) that retains full signaling capability via $G\alpha_q$ (8). This construct lacks all potential phosphorylation sites within ICL3, except two serines and threonines in the N- and C-terminal portions of the loop. We first determined the potency of CCh to induce β-arrestin-2 recruitment to the $M_1\Delta i3$mAChR (Fig. 2*A*). After a 5-min incubation, the pEC_{50} of CCh at this mutant receptor was not significantly different to WT. However, despite comparable CCh affinity and cell surface expression (data not shown), maximum recruitment to the $M_1\Delta i3$mAChR was only one-fifth of the WT E_{max}.

Interestingly, the rate of β-arrestin-2 recruitment to this truncated receptor was also different from that observed at the WT receptor, with a slow onset and no obvious plateau reached even after 20 min (Fig. 2*B*). To gain a better understanding of the dynamics of the β-arrestin-2 interaction with WT and Δi3receptors, we measured the BRET signal after prolonged incubation with 1 mM CCh in the presence of cycloheximide (Fig. 2*C*). The CCh-induced BRET signal between WT M_1-Rluc8 and YFP-β-arrestin-2 started to decline after 20 min and had reached base-line levels by 60 min. In contrast, the association of $M_1\Delta i3$-Rluc8 with YFP-β-arrestin-2 was maintained for at least 2 h despite the limited initial recruitment of YFP-β-arrestin-2. These results thus suggest that the ICL3 of the M_1 mAChR contains the key components that determine the dynamics of the interaction with β-arrestin-2.

In family A GPCRs, the conserved (E/D)RY motif at the intracellular end of transmembrane domain III is critical for G protein activation (25). Mutation of the arginine residue within this motif at the M_3 mAChR compromised G protein activation but not β-arrestin recruitment (26). We, therefore, investigated the effect of the equivalent mutation at the M_1 mAChR. The $R123^{3.50}L$ M_1 mAChR exhibited severely compromised signaling via $G\alpha_q$ as revealed by a large rightward shift in the CCh concentration-response curve for calcium mobilization (Fig. 3*A*), confirming the role of this residue in G protein coupling to M_1 mAChRs. However, in contrast to the observations at the M_3 mAChR, β-arrestin-2 recruitment to the M_1R123L mAChR was also significantly reduced when compared with wild type. The effect of such a mutation was observed as both a reduction in CCh efficacy (Fig. 3*B*) as well as shortened duration of the association of the receptor with YFP-β-arrestin-2 (Fig. 3*C*). Such impaired arrestin recruitment was not due to reduced receptor expression, as [^{3}H]NMS saturation binding was comparable with wild type (data not shown). These results together with the UBO-QIC inhibitor effect confirm that β-arrestin recruitment at the M_1 mAChR depends on G protein activation.

CCh-induced M_1 mAChR Internalization—β-Arrestins have classically been implicated in GPCR signal termination and internalization. We used an anti-myc ELISA on whole cells to identify cell surface c-myc-M_1 mAChRs remaining after incubation with ligand at 37 °C (in the presence of the *de novo* protein synthesis inhibitor cycloheximide). CCh induced a concentration and time-dependent loss of surface receptors to a maximum of ~30% after 4 h (Fig. 4*A*). Hypertonic sucrose and the clathrin terminal domain inhibitor, Pitstop 2 (27), prevented CCh-induced internalization of the c-myc-M_1 mAChR (Fig. 4*B*). However, when cells were pretreated with the dynamin I/II inhibitor dynasore (28), we could not detect a significant effect of this inhibitor on M_1 mAChR internalization (Fig. 4*B*).

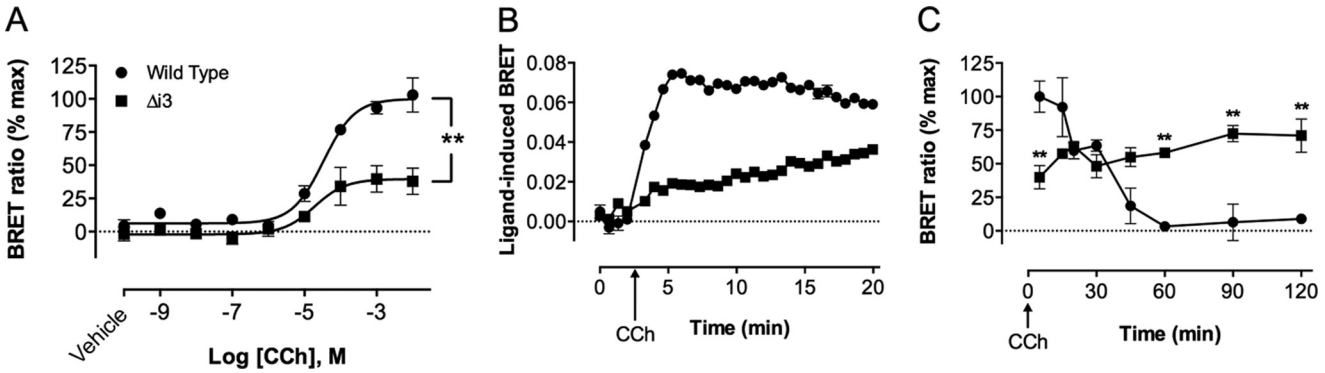

FIGURE 2. **Role of M_1 mAChR ICL3 in β-arrestin recruitment.** *A*, β-arrestin-2 BRET concentration-response curves measured after incubation with ligand for 5 min with WT (*circles*) or Δi3 (*squares*) M_1-Rluc8. $n = 4$. The *asterisk* indicates a significantly different E_{max} (**, $p < 0.01$). *B*, kinetics of β-arrestin-2 BRET at the WT or Δi3 M_1 mAChR after the addition of 1 mM CCh (*arrow*). Kinetic profiles are a representative experiment from $n = 2$. *C*, dissociation of β-arrestin-2 from the WT or Δi3 M_1 mAChR in the continued presence of 1 mM CCh (added at time 0) and 10 μg/ml cycloheximide. $n = 2$. *Asterisks* denote a significant difference in BRET signal (**, $p < 0.01$).

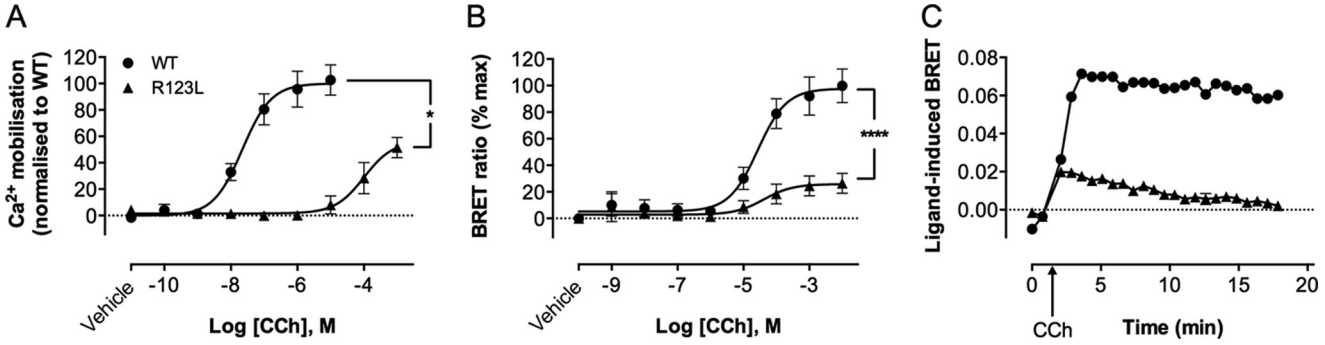

FIGURE 3. **G protein coupling is required for M_1 mAChR-mediated β-arrestin recruitment.** *A*, concentration-response curves of CCh-mediated calcium mobilization by the WT (*circles*) or R123L (*triangles*) M_1 mAChR, stably expressed in FlpIn CHO cells. $n = 3$. The *asterisk* indicates a significantly different E_{max} (*, $p < 0.05$). *B*, β-arrestin-2 BRET concentration-response curves measured after incubation with ligand for 5 min. $n = 5$. *Asterisks* indicate a significantly different E_{max} (****, $p < 0.0001$). *C*, kinetics of β-arrestin-2 BRET at the WT or R123L M_1 mAChR after addition of 1 mM CCh (*arrow*). Kinetic profiles are a representative experiment from $n = 2$.

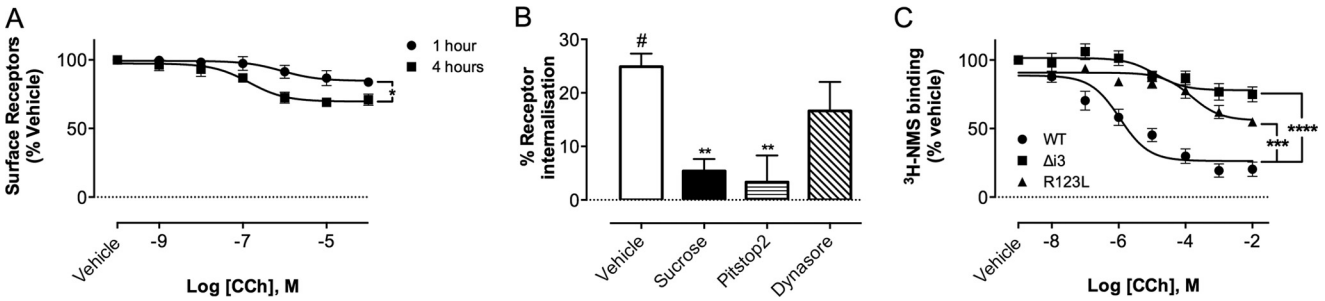

FIGURE 4. **CCh-induced internalization of wild type and mutant M_1 mAChR.** *A*, concentration-response curves of CCh-induced M_1 mAChR internalization after 1 or 4 h. Surface receptors were detected by anti-myc ELISA. $n = 3$. *B*, effect of clathrin (sucrose, Pitstop2) and dynamin (Dynasore) inhibition on CCh-induced M_1 internalization. Cells were incubated with 10 μM CCh for 4 h in the absence (*Vehicle*) or presence of 0.4 M sucrose, 80 μM Pitstop 2, or 30 μM Dynasore. Surface receptors were detected by anti-myc ELISA. $n = 3–6$. *Asterisks* indicate a significant difference compared with vehicle (**, $p < 0.01$). *C*, concentration-response curves of CCh-mediated internalization at the WT, Δi3, or R123L M_1 mAChR, detected using whole cell radioligand binding. $n = 6–10$. *Asterisks* indicate significantly different E_{max} values compared with WT (***, $p < 0.001$; ****, $p < 0.0001$). There is a significant difference in pEC_{50} between WT and R123L ($p < 0.01$) and between WT and Δi3 ($p < 0.05$).

As both the M_1R123L and M_1Δi3 receptors exhibited severely compromised β-arrestin-2 recruitment, we used them as tools to investigate the role of this scaffolding protein in M_1 mAChR internalization. After a 4-h incubation with increasing concentrations of CCh, both mutant receptors exhibited reduced maximum internalization compared with WT as detected with [^{3}H]NMS binding (Fig. 4*C*). The potency of CCh at both mutants was also significantly reduced compared with WT. Because the internalization results mirror the ability of each receptor to recruit β-arrestin-2, they suggest that β-arrestin recruitment plays a key role in the internalization of the M_1 mAChR.

BQCA Is a Positive Allosteric Modulator of M_1 mAChR Signaling and β-Arrestin-2 Recruitment—The ability of BQCA to potentiate the acute responses to CCh was investigated in cells stably expressing the M_1 mAChR. Inositol 1-phosphate accumulation was used as a canonical measure of M_1 mAChR activation resulting from preferential activation of $G\alpha_q$ proteins. As expected, BQCA robustly potentiated CCh-mediated inositol 1-phosphate accumulation in a concentration-dependent

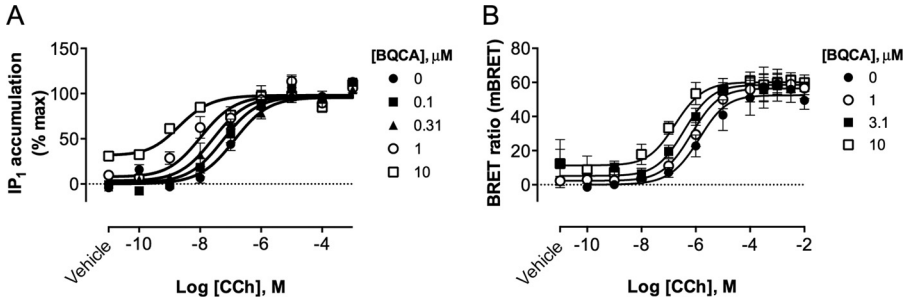

FIGURE 5. **BQCA is a positive allosteric modulator of M_1 mAChR signaling and β-arrestin recruitment.** *A*, BQCA potentiates CCh-mediated inositol 1-phosphate (IP_1) production by the M_1 mAChR and displays agonism at the highest concentration tested. $n = 3$. Curves drawn through the points represent the best fit of the operational model of allosterism and agonism (Equation 1). *B*, interaction between CCh and BQCA in YFP-β-arrestin-2 BRET with hM_1-Rluc8. $n = 4$. Curves drawn through the points represent the best fit of the operational model of allosterism and agonism (Equation 1). *mBRET*, milliBRET units.

TABLE 1

Allosteric parameters for the functional interaction between CCh and BQCA at the M_1 mAChR

Parameter values represent the mean ± S.E. from 3–4 experiments performed in duplicate and analyzed according to Equation 1. IP_1, inositol 1-phosphate.

Parameter	IP_1	β-Arrestin-2
pK_B[a]	3.98	3.98
Log $\alpha\beta$[b]	3.16 ± 0.16 ($\alpha\beta$ = 1445)	2.14 ± 0.18 ($\alpha\beta$ = 138)
Log τ_B[c]	0.63 ± 0.17	0.24 ± 0.25

[a] Negative logarithm of the equilibrium dissociation constant of BQCA; value was fixed to that determined from radioligand binding assays at the wild type M_1 mAChR (8).
[b] Logarithm of the product of the binding cooperativity (α) and activation modulation (β) factors between CCh and BQCA. The anti-logarithm is shown in parentheses.
[c] Logarithm of the operational efficacy parameter of BQCA as an allosteric agonist.

TABLE 2

Effect of BQCA on CCh-induced β-arrestin recruitment at WT, Δi3, and R123L M_1 mAChRs

Potency (pEC_{50}) and E_{max} values are the mean ± S.E. from 3–7 experiments performed in triplicate.

Receptor	CCh alone		CCh + 10 μM BQCA	
	pEC_{50}	E_{max}	pEC_{50}	E_{max}
WT	4.54 ± 0.06	57.01 ± 4.72	6.23 ± 0.28[a]	66.05 ± 7.23
Δi3	4.59 ± 0.18	22.73 ± 6.13[b]	6.21 ± 0.26[c]	27.07 ± 5.65[b]
R123L	4.15 ± 0.32	14.52 ± 3.72[d]	5.36 ± 0.24[e]	18.90 ± 5.44[d]

[a] Significant effect of BQCA: $p < 0.0001$.
[b] Significant difference from WT: $p < 0.01$.
[c] Significant effect of BQCA: $p < 0.01$.
[d] Significant difference from WT: $p < 0.0001$.
[e] Significant effect of BQCA: $p < 0.05$.

manner. In addition, and as previously described, BQCA displayed moderate agonism on its own (Fig. 5*A*, Table 1).

We then tested the effect of BQCA on the recruitment of β-arrestin-2 to the M_1 mAChR. BQCA on its own did not induce significant β-arrestin-2 recruitment to the wild type receptor (Fig. 5*B*). However, in agreement with its modulatory activity, BQCA potentiated the effect of CCh on β-arrestin-2 recruitment (estimated allosteric parameters shown in Table 1). These results demonstrate that BQCA positively modulates the recruitment of β-arrestin-2 to the M_1 mAChR.

We also investigated whether BQCA was able to potentiate β-arrestin-2 recruitment at the mutant M_1 mAChRs that lacks ICL3 or show compromised G protein coupling. As shown in Table 2, co-incubation of CCh with 10 μM BQCA induced the same degree of modulation at both mutants, which was similar to the potentiation observed at the wild type receptor, without changes in the E_{max}.

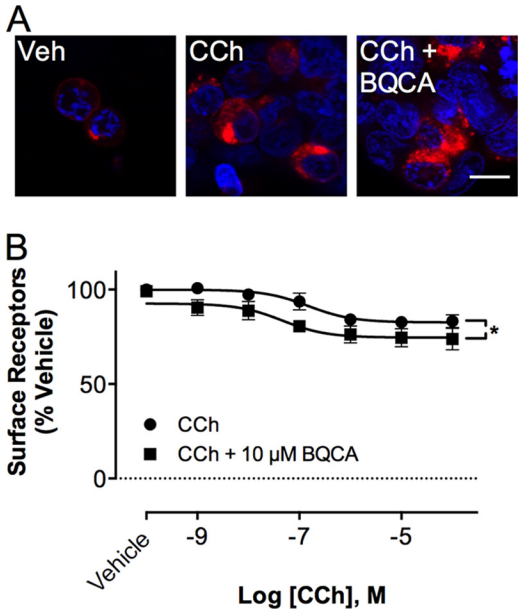

FIGURE 6. **Effect of BQCA on M_1 mAChR internalization.** *A*, cells expressing c-myc-M_1 mAChR were incubated for 4 h with or without ligands (10 μM), washed, and then processed for immunocytochemistry. Photomicrographs show anti-myc-M_1 mAChR immunostaining (*red*) and Hoechst 33342 nuclear stain (*blue*). c-myc-M_1 mAChR was present largely at the plasma membrane in untreated cells. c-myc-M_1 mAChR immunostaining in CCh-treated cells was localized in punctate, vesicular structures. Similarly, in cells treated with CCh + BQCA, c-myc-M_1 mAChR immunostaining was punctate, with little plasma membrane localization. The *scale bar* (10 μm) applies to all photomicrographs. *B*, CCh-mediated M_1 mAChR internalization was increased after co-incubation with 10 μM BQCA. Surface receptors were detected by anti-myc ELISA. $n = 4$. The *asterisk* indicates significantly different E_{max} (*, $p < 0.05$).

Effects of BQCA on Endocytic Trafficking of the M_1 mAChR—To further investigate the fate of M_1 mAChRs upon incubation with CCh with or without BQCA, we used immunocytochemistry and sequential confocal imaging. In unstimulated HEK293 cells, c-myc-M_1 mAChRs were largely localized at the plasma membrane (Fig. 6*A*). In contrast, stimulation of M_1 mAChRs with CCh or CCh and BQCA (10 μM each) induced receptor endocytosis to intracellular vesicles (Fig. 6*A*). Using whole cell ELISA, when cells expressing c-myc-M_1 mAChR were co-incubated with 10 μM BQCA for 1 h, we could not detect a significant change in the potency of CCh (Fig. 6*B*). There was, however, a significant increase in the maximum degree of internalization.

To quantitatively assess receptor internalization and subcellular location upon agonist stimulation, we used a recently

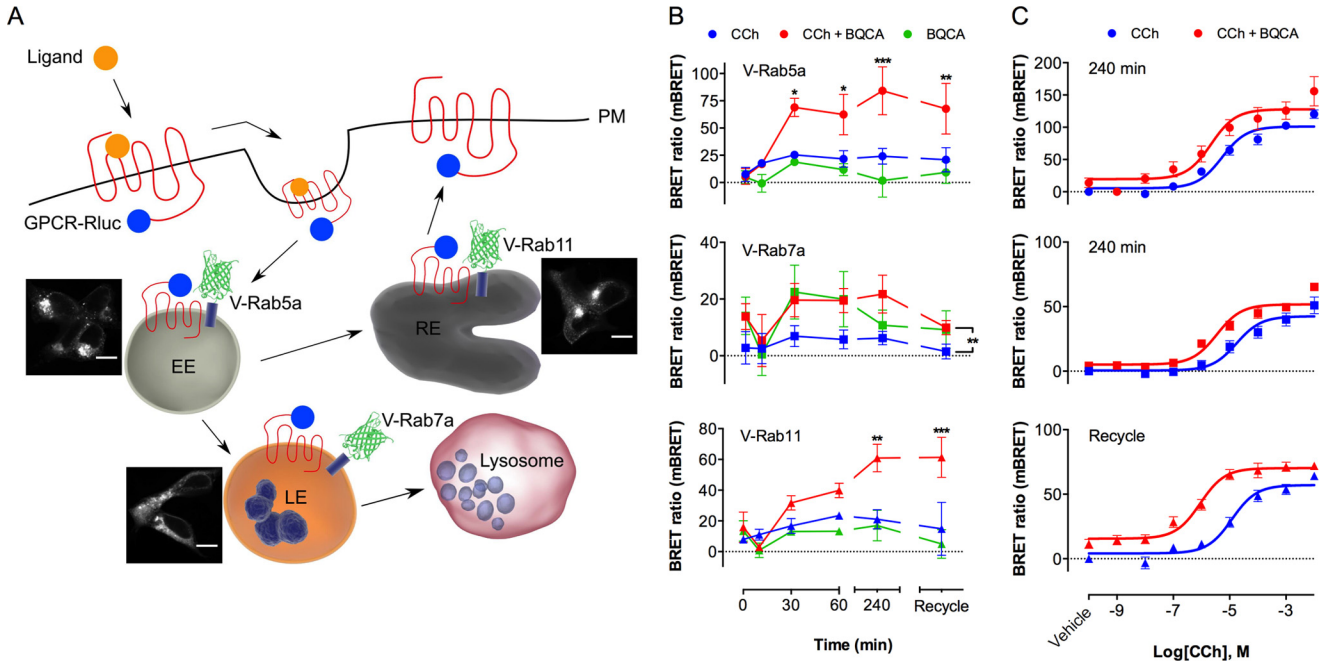

FIGURE 7. **Effect of BQCA on endosomal trafficking of the M_1 mAChR.** *A*, locations of membrane compartment markers used in the BRET internalization assay. The diagram illustrates the classical pathway of GPCR endocytosis, with the location of the three Venus-tagged markers indicated. After ligand binding, the Rluc8-tagged receptor is internalized and transits to the $Rab5a^+$ early endosome (*EE*). Receptors are then trafficked to $Rab11^+$ recycling endosomes (*RE*) for resensitization at the plasma membrane (*PM*). Alternatively, the early endosome matures to form $Rab7a^+$ late endosomes (*LE*) in preparation for cargo degradation in the lysosome. *Insets* adjacent to each compartment show photomicrographs, obtained using a confocal microscope, of HEK293 cells transiently transfected with the corresponding Venus-tagged marker. *Scale bars*, 10 μm. *B*, endosomal trafficking of the M_1 mAChR in response to 10 μM CCh (*blue*), 10 μM CCh + 10 μM BQCA (*red*), or 10 μM BQCA (*green*). Cells were incubated with ligands for up to 4 h or incubated for 4 h and, after washing, incubated for a further 2 h in ligand-free media ("recycle"). Each graph shows BRET measurements taken from cells transfected with hM_1-Rluc8 and either Venus (V)-Rab5a (*top*), V-Rab7a (*middle*), or V-Rab11 (*bottom*). Measurements were acquired in end-point mode. $n = 3–4$. *Asterisks* indicate significant difference between CCh and CCh + BQCA treatments (*, $p < 0.05$; **, $p < 0.01$; ***, $p < 0.001$). *C*, concentration-response curves for CCh in the absence (*blue*) or presence (*red*) of 10 μM BQCA at the indicated time points. BRET pairs are graphed in the same order as in *B*. $n = 4$. *mBRET*, milliBRET units.

described BRET assay that allows the detection of energy transfer between receptors and BRET partners targeted to defined subcellular compartments in live cells (15, 29, 30). M_1-Rluc8 was co-expressed in HEK293 cells with one of three Venus-tagged BRET acceptors localized to different subcellular compartments: Venus-Rab5a in early endosomes, Venus-Rab7a in late endosomes/lysosomes, and Venus-Rab11 in recycling endosomes (Fig. 7*A*). Cells were incubated with CCh or CCh plus BQCA (both at 10 μM) at 37 °C in the presence of cycloheximide to prevent *de novo* protein synthesis. BRET was measured after 0–4 h in the presence of ligands. Alternatively, BRET was measured after a combination of 4-h ligand incubation, thorough washing, and 2 h in the absence of ligand to investigate receptor recycling. This washing protocol resulted in complete removal of ligand (data not shown). The Rluc substrate coelenterazine h was added in the last 10 min of agonist incubation before BRET measurements.

Incubation of M_1-Rluc8-expressing cells with CCh led to a significant increase in BRET signal with Venus-Rab5a or Venus-Rab11 within 10 min (Fig. 7*B*, *top* and *bottom panels*). Both Rab5a and Rab11 BRET showed a trend to return to base line 2 h after CCh washout. In contrast, Rab7a BRET remained close to base-line levels throughout the CCh incubation period (Fig. 7*B*, *middle panel*). These findings suggest internalized M_1 mAChRs rapidly enter the early and recycling endosome pools upon activation, whereas transit into lysosomes occurs only after prolonged ligand incubation.

The addition of BQCA alone (10 μM) to M_1-Rluc8-transfected cells increased BRET in the Rab5a- and Rab11-transfected cells but only at 30 and 60 min, respectively (Fig. 7*B*). Interestingly, co-addition of CCh and BQCA resulted in a significant increase in the BRET signal in all three compartments. It is important to note that the effect of BQCA on CCh-induced BRET can only be assessed at one donor-acceptor pair (31). Differences between two different BRET pairs cannot be evaluated due to the potential effects of protein conformations and dipole orientations discussed above. As such, the smaller increase in ligand-induced BRET between M_1-Rluc8 and Venus-Rab7a, compared with the other Rab markers, does not necessarily mean a smaller effect on trafficking to this compartment.

To rule out simple additive agonism as the cause of the increased ligand-induced BRET signal, we constructed concentration-response curves for CCh in the absence or presence of 10 μM BQCA. We measured ligand-induced BRET after 4 h for Rab5a and Rab7a or after ligand washout for Rab11 (Fig. 7*C*). In contrast to the ELISA for surface receptors, we could detect significant modulation by BQCA. BQCA increased the potency of CCh-mediated M_1-Rluc8 BRET with Rab5a (2.4-fold), Rab7a (5-fold), and Rab11 (13-fold) with negligible agonism. These data confirm that BQCA acts as a positive allosteric modulator at the level of M_1 mAChR trafficking.

Taken together these results support the hypothesis that BQCA potentiates CCh-induced M_1 mAChR internalization. Our BRET results show that BQCA has a significant impact on

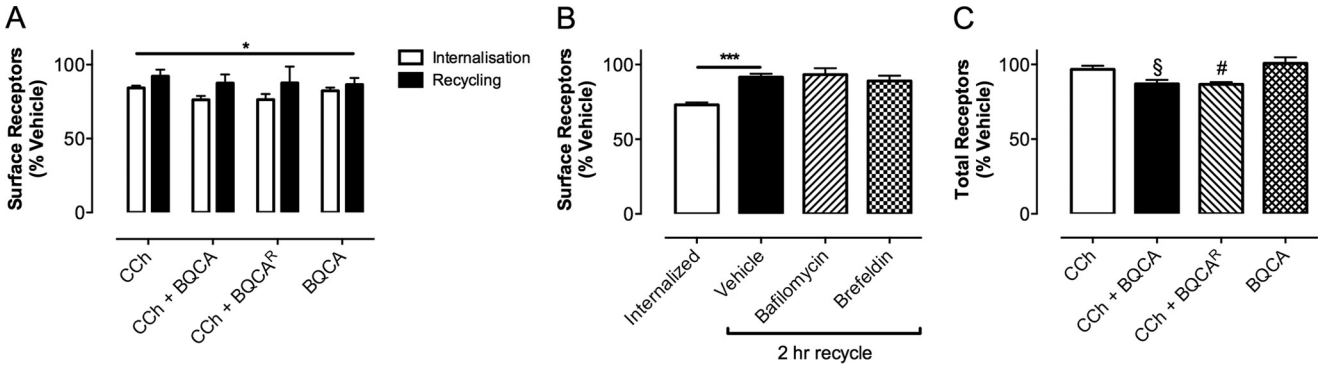

FIGURE 8. **Fate of the M_1 mAChR after endocytosis.** *A*, cells were incubated with ligand for 4 h, washed, and incubated in the absence of ligand for 2 h. Recycling was evident after CCh, CCh + BQCA, and CCh + $BQCA^R$ (BQCA also present during recycling) treatments but not after BQCA alone (all 10 μM). $n = 4–7$. The *asterisk* indicates main effect of recycling (*, $p < 0.05$). *B*, recycling of M_1 receptors to the cell surface is not bafilomycin- or brefeldin-sensitive. After a 4-h incubation with 10 μM CCh (*Internalized*), cells were washed and incubated for 2 h in the absence (*vehicle*) or presence of bafilomycin A1 (10 μM) or brefeldin A (1 μg/ml). Surface receptors were detected by anti-myc ELISA. $n = 3–6$. *Asterisks* denote a significant effect of washout on surface receptor density (***, $p < 0.001$). *C*, degradation of M_1 receptors was evident after washout of CCh + BQCA but not CCh or BQCA alone. Cells were treated as in *A*, and total receptors remaining after the 2-h washout period were detected by anti-myc ELISA in permeabilized cells. $n = 3–6$. *Symbols above the bars* indicate a significant difference compared with vehicle treatment (#, $p < 0.05$; §, $p < 0.01$).

endosomal trafficking dynamics of the M_1 mAChR and also highlight the utility of this sensitive resonance energy transfer approach to delineate such receptor regulatory events.

BQCA Modulates M_1 mAChR Recycling and Degradation—Once internalized, GPCRs can be recycled back to the plasma membrane or sorted to lysosomal compartments and subsequent degradation. As we detected the presence of M_1 mAChR in $Rab11^+$ (recycling) endosomes upon removal of ligand (Fig. 7*B*), we investigated whether M_1 mAChRs returned to the plasma membrane after agonist removal.

Surface receptors were detected using the anti-myc ELISA. CCh with or without 10 μM BQCA was applied to cells for 4 h followed by agonist washout and a further 2-h incubation in the absence of ligand. As shown previously, incubation with all ligands for 4 h led to a significant reduction in surface receptor levels compared with vehicle (Fig. 8*A*). Removal of the ligand resulted in an overall increase of surface receptor levels, except for treatment with BQCA alone, which remained at the pre-washout level. These results support the previous BRET results and confirm that the M_1 mAChR recycles to the cell surface upon agonist removal. However, we were unable to inhibit M_1 mAChR recycling using either the vacuolar H^+-ATPase inhibitor bafilomycin A1 or the protein secretion inhibitor brefeldin A (Fig. 8*B*), indicating that neither endosome acidification nor Golgi function was required for the return of M_1 mAChR to the plasma membrane.

The presence of M_1 mAChRs in the Rab7a subcellular compartment (Fig. 7*B*) suggested that some M_1 mAChRs might be targeted to the late endosomes/lysosomes. We, therefore, investigated the extent of receptor degradation after different ligand combinations using a whole cell anti-myc ELISA on permeabilized cells, which allowed us to detect total receptors (32). Although the total amount of receptors was not affected after incubation with CCh or BQCA alone followed by ligand washout, a significant decrease was observed after washout of CCh and BQCA as well as when BQCA was maintained in the recovery media (Fig. 8*C*). These results are in agreement with our previous results and suggest that the proportion of M_1 mAChRs that traffic to lysosomes is increased upon incubation of CCh with BQCA.

DISCUSSION

Because of their improved receptor subtype selectivity, allosteric ligands represent an attractive approach for the development of novel therapies. However, as the net effect of any receptor-based therapy reflects the interplay between acute signaling and longer term regulatory pathways, it is crucial to understand not only the acute but also the chronic effects of allosteric drugs at their corresponding GPCR target (11). M_1 mAChR allosteric modulators have been proposed as potential therapeutics for various CNS disorders (33). However, our understanding of their effects on receptor regulatory processes such as receptor internalization and subcellular trafficking is still limited. In the current study we have evaluated these effects for the M_1 mAChR allosteric modulator BQCA, which is an unprecedented example of an allosteric modulator with very high selectivity and positive cooperativity with ACh at the M_1 mAChR (6, 8). Pharmacologically, BQCA displays simple receptor "state dependence" and does not engender stimulus bias (8, 17), in contrast to previously reported mAChR allosteric modulators such as LY2033298 (10). As such, BQCA is an ideal chemical tool with which to assess how allosteric ligands can affect receptor levels and trafficking dynamics in a model system. Our results show that in heterologously expressing cells, M_1 mAChRs recruit β-arrestins and internalize upon agonist stimulation. BQCA positively modulates β-arrestin recruitment to the M_1 mAChR and potentiates subcellular trafficking of the receptor via the different endocytic compartments.

The role of β-arrestins in mAChR regulation has been explored previously, and it was suggested that although both isoforms (β-arrestin-1 and -2) were implicated in M_1 mAChR regulation (34), they were not required for receptor internalization (35). We show that the M_1 mAChR recruits β-arrestins 1 and 2 within minutes of its activation by CCh. Recruitment of β-arrestin-2 occurs via a mechanism that involves, at least partially, the kinase activity of GRK2. Additionally, using β-arres-

tin recruitment-compromised M_1 mAChR mutants (Δi3 and R123L), our results suggest that binding of this scaffolding protein to the activated receptor is necessary for internalization. Importantly, our results also emphasize two mechanistic features of M_1 mAChR regulation. First, the dynamics of the interaction between β-arrestin-2 and the M_1 mAChR may be dictated by other proteins that also bind to ICL3, suggesting a potential mechanism for the previous observations of compromised internalization of truncated M_1 mAChRs (36). Second, recruitment of β-arrestin to the M_1 mAChR requires G protein activation, as abrogating G protein coupling to the receptor has a significant impact not only on arrestin recruitment but also on receptor internalization, which is different from observations at the M_3 mAChR (26).

BQCA has been described as a positive allosteric modulator based on its effects on the actions of ACh in canonical signaling pathways linked to M_1 mAChR activation. Our study shows that this behavior extends to potentiation of β-arrestin recruitment and endocytic trafficking. Interestingly, we did not detect substantial allosteric agonism by BQCA in the β-arrestin recruitment BRET assay. This latter result aligns with the previous descriptions of BQCA behavior in that β-arrestin recruitment is a very proximal event to receptor activation subject to minimal amplification. Because the degree of direct agonism in the actions of BQCA is primarily a function of cellular stimulus-response coupling efficiency, it is anticipated that little or no agonism of BQCA would be detected when measuring β-arrestin recruitment (8). This expectation is also applicable to other regulatory processes such as internalization and endocytic trafficking. Moreover, the effect of BQCA on M_1 mAChR mutants with compromised internalization also aligns with previous observations that establish BQCA as an allosteric modulator whose effects are mainly mediated by positive cooperativity of receptor affinity and limited cooperativity in terms of receptor efficacy. In contrast, this is not the case for the M_4 mAChR-selective allosteric ligand, LY2033298, which engenders stimulus bias at the M_4 mAChR, whereby the degree of potentiation does not track with the stimulus-response coupling efficiency and, therefore, allows for more complex agonistic behaviors (10).

Once internalized, receptors can be directed to degradative pathways (receptor down-regulation) or recycled back to the cell surface (37). Receptor trafficking through the endocytic machinery as well as the fate of internalized receptors is agonist-dependent (38–40). Using a novel quantitative BRET approach (15, 29) we show for the first time the subcellular trafficking of the M_1 mAChR upon CCh stimulation. This approach provides a complementary method to immunocytochemistry and allows for the quantification of ligand-dependent effects on receptor trafficking (15, 29). Within 10 min of CCh incubation, M_1 mAChRs trafficked into $Rab5^+$ early endosomes and $Rab11^+$ recycling endosomes. Co-incubation of CCh with BQCA had a marked effect on the trafficking of the M_1 mAChR. Although it did not change the trafficking profile, BQCA increased the BRET signal from receptors localized within the different subcellular compartments, especially Rab5a- and Rab11-containing endosomes. Moreover, this effect is due to an increase in CCh potency at all three BRET pairs, ruling out a simple additive effect. Therefore, although we could not detect BQCA-induced modulation of internalization of the WT M_1 mAChR using whole cell ELISA, more sensitive approaches such as BRET allow us for the first time to assess allosteric modulation of receptor trafficking.

Further validation of the BRET approach is supported by the fact that ELISA experiments performed after agonist washout show the recovery of receptor at the cell surface, which is in agreement with the localization of M_1 mAChRs in $Rab11^+$ endosomes. However, this recycling could not be blocked by inhibitors of endosomal acidification, such as bafilomycin A1, or by Golgi disruption. Hence, alternate mechanisms of receptor recycling may be responsible for M_1 mAChR recovery. Finally, when cells were treated with both CCh and BQCA, BRET between M_1-Rluc8 and Venus-Rab7a decreased after ligand washout, indicative of movement out of this compartment into the lysosome. This suggested that prolonged incubation followed by washout of CCh plus BQCA might lead to increased receptor degradation. This was confirmed using ELISA to detect total receptor expression, which only decreased when cells were incubated with CCh and BQCA and not when either ligand was added individually. These results are in line with our trafficking data and suggest that potentiation of the M_1 mAChR by BQCA increases the relative amount of receptor targeted for degradation.

Allosteric modulators have emerged as promising alternatives for the subtype-selective targeting of GPCRs. Therefore, it will be important to determine how this class of ligands regulates their target GPCR. In addition to BQCA, modulation of mAChR internalization has been demonstrated previously by the mAChR negative allosteric ligand gallamine at the M_2 mAChR and by LY2033298 at the M_4 mAChR. Gallamine decreases CCh-induced M_2 mAChR internalization and up-regulates cell surface receptor levels (41). In contrast, LY2033298 potentiates ACh-induced M_4 mAChR internalization to a greater extent than would be predicted from acute signaling assays, effectively demonstrating a biased action toward regulatory pathways (10). Our results show that in heterologous systems a positive allosteric modulator of the M_1 mAChR also behaves as such with regard to receptor regulation without evidence of bias. However, this remains to be validated in more physiologically relevant systems. Unfortunately, to our knowledge there are no neuronal cell lines validated for the study of endogenous M_1 mAChRs. In addition, the lack of reliable M_1 mAChR specific antibodies is a significant obstacle to the evaluation of the trafficking of these receptors in primary neuronal cultures. Development of more subtype selective probes to investigate mAChR trafficking will be of great significance to translate our findings into native expression systems.

In summary, the allosteric ligand BQCA modulates M_1 mAChR regulation; it enhances β-arrestin recruitment and receptor trafficking to intracellular endocytic compartments. This has significant therapeutic implications when considering prolonged exposure to this new class of ligands.

Acknowledgments—We thank Marc Caron (Duke University) for the YFP-β-arrestin-1 and -2 constructs and Jurgen Wess (NIDDK, National Institutes of Health) for the p416GPD-M_1Δi3 construct.

REFERENCES

1. Langmead, C. J., Watson, J., and Reavill, C. (2008) Muscarinic acetylcholine receptors as CNS drug targets. *Pharmacol. Ther.* **117,** 232–243
2. Davie, B. J., Christopoulos, A., and Scammells, P. J. (2013) Development of M1 mAChR allosteric and bitopic ligands: prospective therapeutics for the treatment of cognitive deficits. *ACS Chem. Neurosci.* **4,** 1026–1048
3. Caulfield, M. P., and Birdsall, N. J. (1998) International Union of Pharmacology. XVII. Classification of muscarinic acetylcholine receptors. *Pharmacol. Rev.* **50,** 279–290
4. Anagnostaras, S. G., Murphy, G. G., Hamilton, S. E., Mitchell, S. L., Rahnama, N. P., Nathanson, N. M., and Silva, A. J. (2003) Selective cognitive dysfunction in acetylcholine M1 muscarinic receptor mutant mice. *Nat. Neurosci.* **6,** 51–58
5. Messer, W. S. (2002) The utility of muscarinic agonists in the treatment of Alzheimer's disease. *J. Mol. Neurosci.* **19,** 187–193
6. Ma, L., Seager, M. A, Seager, M., Wittmann, M., Jacobson, M., Bickel, D., Burno, M., Jones, K., Graufelds, V. K., Xu, G., Pearson, M., McCampbell, A., Gaspar, R., Shughrue, P., Danziger, A., Regan, C., Flick, R., Pascarella, D., Garson, S., Doran, S., Kreatsoulas, C., Veng, L., Lindsley, C. W., Shipe, W., Kuduk, S., Sur, C., Kinney, G., Seabrook, G. R., and Ray, W. J. (2009) Selective activation of the M1 muscarinic acetylcholine receptor achieved by allosteric potentiation. *Proc. Natl. Acad. Sci. U.S.A.* **106,** 15950–15955
7. Shirey, J. K., Brady, A. E., Jones, P. J., Davis, A. A., Bridges, T. M., Kennedy, J. P., Jadhav, S. B., Menon, U. N., Xiang, Z., Watson, M. L., Christian, E. P., Doherty, J. J., Quirk, M. C., Snyder, D. H., Lah, J. J., Levey, A. I., Nicolle, M. M., Lindsley, C. W., and Conn, P. J. (2009) A selective allosteric potentiator of the M1 muscarinic acetylcholine receptor increases activity of medial prefrontal cortical neurons and restores impairments in reversal learning. *J. Neurosci.* **29,** 14271–14286
8. Canals, M., Lane, J. R., Wen, A., Scammells, P. J., Sexton, P. M., and Christopoulos, A. (2012) A Monod-Wyman-Changeux mechanism can explain G protein-coupled receptor (GPCR) allosteric modulation. *J. Biol. Chem.* **287,** 650–659
9. Keov, P., Valant, C., Devine, S. M., Lane, J. R., Scammells, P. J., Sexton, P. M., and Christopoulos, A. (2013) Reverse engineering of the selective agonist, TBPB, unveils both orthosteric and allosteric modes of action at the M1 muscarinic acetylcholine receptor. *Mol. Pharmacol.* **84,** 425–437
10. Leach, K., Loiacono, R. E., Felder, C. C., McKinzie, D. L., Mogg, A., Shaw, D. B., Sexton, P. M., and Christopoulos, A. (2010) Molecular mechanisms of action and in vivo validation of an M4 muscarinic acetylcholine receptor allosteric modulator with potential antipsychotic properties. *Neuropsychopharmacology* **35,** 855–869
11. Lane, J. R., Abdul-Ridha, A., and Canals, M. (2013) Regulation of G protein-coupled receptors by allosteric ligands. *ACS Chem. Neurosci.* **4,** 527–534
12. Ferguson, S. S., Downey, W. E., 3rd, Colapietro, A. M., Barak, L. S., Ménard, L., and Caron, M. G. (1996) Role of β-arrestin in mediating agonist-promoted G protein-coupled receptor internalization. *Science* **271,** 363–366
13. Xiao, K., McClatchy, D. B., Shukla, A. K., Zhao, Y., Chen, M., Shenoy, S. K., Yates, J. R., 3rd, and Lefkowitz, R. J. (2007) Functional specialization of β-arrestin interactions revealed by proteomic analysis. *Proc. Natl. Acad. Sci. U.S.A.* **104,** 12011–12016
14. Oakley, R. H., Laporte, S. A., Holt, J. A., Barak, L. S., and Caron, M. G. (1999) Association of β-arrestin with G protein-coupled receptors during clathrin-mediated endocytosis dictates the profile of receptor resensitization. *J. Biol. Chem.* **274,** 32248–32257
15. Lan, T.-H., Liu, Q., Li, C., Wu, G., and Lambert, N. A. (2012) Sensitive and high resolution localization and tracking of membrane proteins in live cells with BRET. *Traffic* **13,** 1450–1456
16. Avlani, V. A., Langmead, C. J., Guida, E., Wood, M. D., Tehan, B. G., Herdon, H. J., Watson, J. M., Sexton, P. M., and Christopoulos, A. (2010) Orthosteric and allosteric modes of interaction of novel selective agonists of the M1 muscarinic acetylcholine receptor. *Mol. Pharmacol.* **78,** 94–104
17. Abdul-Ridha, A., Lane, J. R., Sexton, P. M., Canals, M., and Christopoulos, A. (2013) Allosteric modulation of a chemogenetically modified G protein-coupled receptor. *Mol. Pharmacol.* **83,** 521–530
18. Christopoulos, A. (1998) Assessing the distribution of parameters in models of ligand-receptor interaction: to log or not to log. *Trends Pharm. Sci.* **19,** 351–357
19. Leach, K., Sexton, P. M., and Christopoulos, A. (2007) Allosteric GPCR modulators: taking advantage of permissive receptor pharmacology. *Trends Pharm. Sci.* **28,** 382–389
20. Tsuga, H., Okuno, E., Kameyama, K., and Haga, T. (1998) Sequestration of human muscarinic acetylcholine receptor hm1-hm5 subtypes: effect of G protein-coupled receptor kinases GRK2, GRK4, GRK5, and GRK6. *J. Pharmacol. Exp. Ther.* **284,** 1218–1226
21. Willets, J. M., Nahorski, S. R., and Challiss, R. A. (2005) Roles of phosphorylation-dependent and -independent mechanisms in the regulation of M1 muscarinic acetylcholine receptors by G protein-coupled receptor kinase 2 in hippocampal neurons. *J. Biol. Chem.* **280,** 18950–18958
22. Haga, K., Kameyama, K., Haga, T., Kikkawa, U., Shiozaki, K., and Uchiyama, H. (1996) Phosphorylation of human m1 muscarinic acetylcholine receptors by G protein-coupled receptor kinase 2 and protein kinase C. *J. Biol. Chem.* **271,** 2776–2782
23. Thal, D. M., Yeow, R. Y., Schoenau, C., Huber, J., and Tesmer, J. J. (2011) Molecular mechanism of selectivity among G protein-coupled receptor kinase 2 inhibitors. *Mol. Pharmacol* **80,** 294–303
24. Violin, J. D., and Lefkowitz, R. J. (2007) β-Arrestin-biased ligands at seven-transmembrane receptors. *Trends Pharm. Sci.* **28,** 416–422
25. Rovati, G. E., Capra, V., and Neubig, R. R. (2007) The highly conserved DRY motif of class A G protein-coupled receptors: beyond the ground state. *Mol. Pharmacol.* **71,** 959–964
26. Nakajima, K., and Wess, J. (2012) Design and functional characterization of a novel, arrestin-biased designer G protein-coupled receptor. *Mol. Pharmacol.* **82,** 575–582
27. von Kleist, L., Stahlschmidt, W., Bulut, H., Gromova, K., Puchkov, D., Robertson, M. J., MacGregor, K. A., Tomilin, N., Tomlin, N., Pechstein, A., Chau, N., Chircop, M., Sakoff, J., von Kries, J. P., Saenger, W., Kräusslich, H.-G., Shupliakov, O., Robinson, P. J., McCluskey, A., and Haucke, V. (2011) Role of the clathrin terminal domain in regulating coated pit dynamics revealed by small molecule inhibition. *Cell* **146,** 471–484
28. Macia, E., Ehrlich, M., Massol, R., Boucrot, E., Brunner, C., and Kirchhausen, T. (2006) Dynasore, a cell-permeable inhibitor of dynamin. *Dev. Cell* **10,** 839–850
29. Jensen, D. D., Godfrey, C. B., Niklas, C., Canals, M., Kocan, M., Poole, D. P., Murphy, J. E., Alemi, F., Cottrell, G. S., Korbmacher, C., Lambert, N. A., Bunnett, N. W., and Corvera, C. U. (2013) The bile acid receptor TGR5 does not interact with β-arrestins or traffic to endosomes but transmits sustained signals from plasma membrane rafts. *J. Biol. Chem.* **288,** 22942–22960
30. Lan, T.-H., Kuravi, S., and Lambert, N. A. (2011) Internalization dissociates β2-adrenergic receptors. *PLoS ONE* **6,** e17361
31. Kocan, M., and Pfleger, K. D. (2011) Study of GPCR-protein interactions by BRET. *Methods Mol. Biol.* **746,** 357–371
32. Canals, M., Scholten, D. J., de Munnik, S., Han, M. K., Smit, M. J., and Leurs, R. (2012) Ubiquitination of CXCR7 controls receptor trafficking. *PLoS ONE* **7,** e34192
33. Conn, P. J., Jones, C. K., and Lindsley, C. W. (2009) Subtype-selective allosteric modulators of muscarinic receptors for the treatment of CNS disorders. *Trends Pharm. Sci.* **30,** 148–155
34. Vögler, O., Nolte, B., Voss, M., Schmidt, M., Jakobs, K. H., and van Koppen, C. J. (1999) Regulation of muscarinic acetylcholine receptor sequestration and function by β-arrestin. *J. Biol. Chem.* **274,** 12333–12338
35. Lee, K. B., Pals-Rylaarsdam, R., Benovic, J. L., and Hosey, M. M. (1998) Arrestin-independent internalization of the m1, m3, and m4 subtypes of muscarinic cholinergic receptors. *J. Biol. Chem.* **273,** 12967–12972
36. Lameh, J., Philip, M., Sharma, Y. K., Moro, O., Ramachandran, J., and Sadée, W. (1992) Hm1 muscarinic cholinergic receptor internalization requires a domain in the third cytoplasmic loop. *J. Biol. Chem.* **267,** 13406–13412
37. Jean-Alphonse, F., and Hanyaloglu, A. C. (2011) Regulation of GPCR signal networks via membrane trafficking. *Mol. Cell Endocrinol.* **331,** 205–214
38. Wu, D.-F., Yang, L.-Q., Goschke, A., Stumm, R., Brandenburg, L.-O., Li-

ang, Y.-J., Höllt, V., and Koch, T. (2008) Role of receptor internalization in the agonist-induced desensitization of cannabinoid type 1 receptors. *J. Neurochem.* **104,** 1132–1143

39. Whistler, J. L., Chuang, H. H., Chu, P., Jan, L. Y., and von Zastrow, M. (1999) Functional dissociation of mu opioid receptor signaling and endocytosis: implications for the biology of opiate tolerance and addiction. *Neuron* **23,** 737–746
40. Raote, I., Bhattacharyya, S., and Panicker, M. M. (2013) Functional selectivity in serotonin receptor 2A (5-HT2A) endocytosis, recycling, and phosphorylation. *Mol. Pharmacol.* **83,** 42–50
41. May, L. T., Lin, Y., Sexton, P. M., and Christopoulos, A. (2005) Regulation of M2 muscarinic acetylcholine receptor expression and signaling by prolonged exposure to allosteric modulators. *J. Pharmacol. Exp. Ther.* **312,** 382–390